

10
1-9-96 95 (1)

Recent Results from the SLD Using a Highly Polarized Electron Beam

Tracy Usher

Representing The SLD Collaboration ¹

*Stanford Linear Accelerator Center
Stanford University
Stanford, CA 94309*

ABSTRACT

New results are presented on the fermion asymmetries, A_b and A_c , and the b -branching ratio, R_b , using a data sample of 150,000 Z^0 decays collected by the SLD during 1993 and 1994. The fermion asymmetries exploit the highly polarized electron beam available at the SLC ($63.0\% \pm 1.1\%$ during 1993 and increasing to a preliminary value of $78.2\% \pm 2.0\%$ during 1994) to perform direct measurements of A_b and A_c . The preliminary results obtained are $A_b = 0.82 \pm 0.06(\text{stat}) \pm 0.08(\text{syst})$, $A_c = 0.63 \pm 0.13(\text{stat}) \pm 0.08(\text{syst})$ and $R_b = 0.218 \pm 0.004(\text{stat}) \pm 0.004(\text{syst}) \pm 0.003(R_c)$. In addition, the measurement of $\sin^2 \theta_W^{\text{eff}}$ from the 1993 A_{LR} result is reviewed. The result obtained is $\sin^2 \theta_W^{\text{eff}} = 0.2292 \pm 0.0009(\text{stat}) \pm 0.0004(\text{syst})$.

Presented at Les Rencontres de Physique de la Vallée D'Aoste: Results and Perspectives in Particle Physics, La Thuile, Italy, March 5-11, 1995

¹This work was supported by Department of Energy contracts: DE-FG02-91ER40676 (BU), DE-FG03-92ER40701 (CIT), DE-FG03-91ER40618 (UCSB), DE-FG03-92ER40689 (UCSC), DE-FG03-93ER40788 (CSU), DE-FG02-91ER40672 (Colorado), DE-FG02-91ER40677 (Illinois), DE-AC03-76SF00098 (LBL), DE-FG02-92ER40715 (Massachusetts), DE-AC02-76ER03069 (MIT), DE-FG06-85ER40224 (Oregon), DE-AC03-76SF00515 (SLAC), DE-FG05-91ER40627 (Tennessee), DE-AC02-76ER00881 (Wisconsin), DE-FG02-92ER40704 (Yale); National Science Foundation grants: PHY-91-13428 (UCSC), PHY-89-21320 (Columbia), PHY-92-04239 (Cincinnati), PHY-88-17930 (Rutgers), PHY-88-19316 (Vanderbilt), PHY-92-03212 (Washington); the UK Science and Engineering Research Council (Brunel and RAL); the Istituto Nazionale di Fisica Nucleare of Italy (Bologna, Ferrara, Frascati, Pisa, Padova, Perugia); and the Japan-US Cooperative Research Project on High Energy Physics (Nagoya, Tohoku).

MASTER

DISTRIBUTION OF THIS DOCUMENT IS UNLIMITED

dp

DISCLAIMER

Portions of this document may be illegible in electronic image products. Images are produced from the best available original document.

1 Introduction

During the 1994 run of the SLAC Large Detector (SLD), 100K Z^0 decays were collected with an electron beam polarization of $78.2 \pm 2.0\%$. This has led to significantly more precise asymmetry measurements and has allowed the use of a hemisphere b -tagging technique to obtain a more precise measurement of $R_b = \Gamma(Z^0 \rightarrow b\bar{b})/\Gamma(Z^0 \rightarrow \text{hadrons})$. The longitudinal polarization of the beam allows the left and right handed components of the $Z^0 \rightarrow f\bar{f}$ coupling to be measured separately. Through observations of the $Z^0 \rightarrow f\bar{f}$ decay rates, excluding Bhabhas, for left and right handed beam polarizations, a direct measurement of the electron asymmetry A_e is made. From this, an accurate measurement of the weak mixing angle is obtained. The heavy quark asymmetries are obtained from a double asymmetry. By measuring the difference of the polar angle distribution of the quark decay directions for left and right handed electron beam polarizations, values for A_b and A_c are obtained. Finally, a hemisphere b -tag technique utilizing the 3-D impact parameters of tracks to the measured primary vertex position is used to measure R_b . The accelerator and detector systems are briefly described, followed by details of the individual analyses.

2 Polarized Electron Operation at the SLC

A detailed discussion of spin transport and measurement at the SLAC Linear Collider (SLC) can be found in reference [1]. Longitudinally polarized electrons are generated by photo-emission from a "strained" GaAs cathode. The straining of the cathode removes a degeneracy in the valence band energy levels of the GaAs and, theoretically, allows for electron beam polarizations approaching 100%. The beam polarization of 22% measured during the 1992 SLC/SLD run was increased to 63% in 1993 as a result of introducing this "strained" GaAs cathode. A further increase in 1994 to 78% was obtained through optimization of the thickness and quality of the GaAs and GaAsP layers of the cathode.

As the electron bunch enters the SLC Damping Ring (needed to reduce the transverse phase space of the bunch) the spins are rotated to the vertical in order to preserve polarization during the 8 ms damping time. Spin orientation remains vertical during re-injection into the LINAC and during acceleration to 46.6 GeV. The electron beam is transported from the end of the LINAC to the SLD Interaction Point (IP) through the north SLC Arc. During this transport the spin orientation is rotated to longitudinal by taking advantage of the coupling of the electron spin precession with the Betatron phase advance of the achromats comprising the arc.

The longitudinal electron polarization is measured by a Compton scattering polarimeter located 33 m downstream of the SLD IP. After passing through the SLD IP, the electron beam collides with a Nd:YAG laser beam of wavelength 532nm. A dipole bending magnet disperses the scattered electrons horizontally into a nine channel Cherenkov detector, which measures their momentum spectrum in the interval from 17 to 30 GeV/c. The electron beam polarization is determined from the asymmetry formed from counts of parallel and anti-parallel combinations of laser beam

and electron beam helicities. Electron polarization is monitored continuously during operation of the SLC with a statistical precision obtained over a three minute interval of 1%.

3 The SLD

Observations of the Z^0 decay products are made using the SLD. The SLD[2] consists of a Warm Iron Calorimeter (WIC) for muon identification; a Liquid Argon Calorimeter(LAC) for measuring energy flow; a Cherenkov Ring Imaging Detector (CRID) for particle identification; a Drift Chamber (CDC) for charged track identification and momentum measurements; and a CCD pixel Vertex Detector (VXD) for precise position measurements near the interaction point.

The calorimetry and tracking systems are used by the analyses presented here and will be briefly discussed (reference [3] contains a detailed description). The LAC barrel covers $|\cos\theta| < 0.84$ and endcaps cover $0.82 < |\cos\theta| < 0.98$ for the full azimuthal range. The electromagnetic energy resolution of the calorimeter barrel is measured to be $\sigma/E = 15\%/\sqrt{E(\text{GeV})}$. The hadronic energy resolution is $60\%/\sqrt{E(\text{GeV})}$. The CDC covers the azimuthal range $|\cos\theta| < 0.72$. Charged tracks are reconstructed in the CDC, linked with pixel clusters in the VXD, and then a combined fit performed. The angular errors of the CDC combined with local errors $\sigma(r\phi)$ and $\sigma(rz)$ of $\sim 6\mu\text{m}$ for the VXD clusters, lead to an $r\phi$ (plane perpendicular to the e^+e^- beam axis) impact parameter resolution of $(\alpha, \beta)_{r\phi} = (11\mu\text{m}, 70\mu\text{m})$. The rz (plane containing the beam axis) impact parameter resolution is $(\alpha, \beta)_{rz} = (38\mu\text{m}, 70\mu\text{m})$. The combined fit momentum resolution is $\delta p_{\perp}/p_{\perp} = 0.01 \oplus 0.0026 p_{\perp}$ (p_{\perp} in GeV/c).

4 R_b Measurement using a Lifetime Double Tag

Measurement of the ratio of the partial width of $Z^0 \rightarrow b\bar{b}$ to the partial width of $Z^0 \rightarrow \text{hadrons}$ (R_b) allows a direct measurement of vertex corrections to the $Zb\bar{b}$ vertex to be made. Due to the increase of the SLD data sample in 1994 we can now employ a double tag technique which greatly reduces the sensitivity of the R_b measurement to the simulation of b -decays and the detector. The measurement is performed in a manner similar to that outlined by ALEPH[4]. To tag a hemisphere one starts by forming a probability that each track is consistent with coming from the primary vertex. This is done by using the 3-D normalized impact parameters (δ) of the tracks. This quantity is signed negative if the point of closest approach between the track and the jet axis is behind the measured primary vertex position. The distribution of $\delta < 0$, shown in Fig. 1, indicates good simulation of the resolutions. A resolution function(R) is parameterized to fit the $\delta < 0$ distribution of tracks in uds events. From this, the integral probability that a track is consistent with coming from the primary vertex position is determined. Then, these probabilities are combined to form the integral probability that the collection of tracks in a hemisphere are

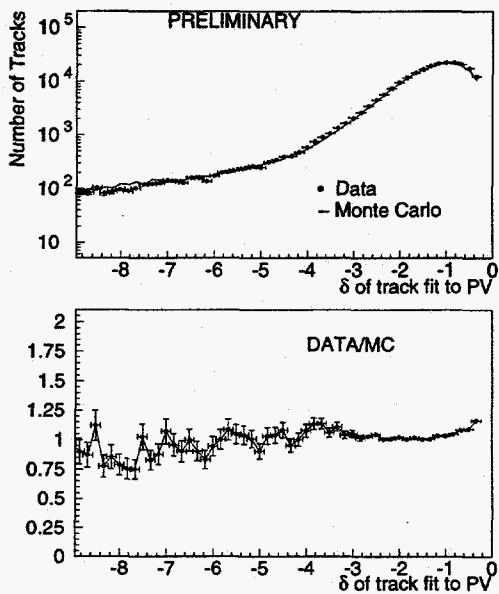


Figure 1: Distribution of δ in data and Monte Carlo.

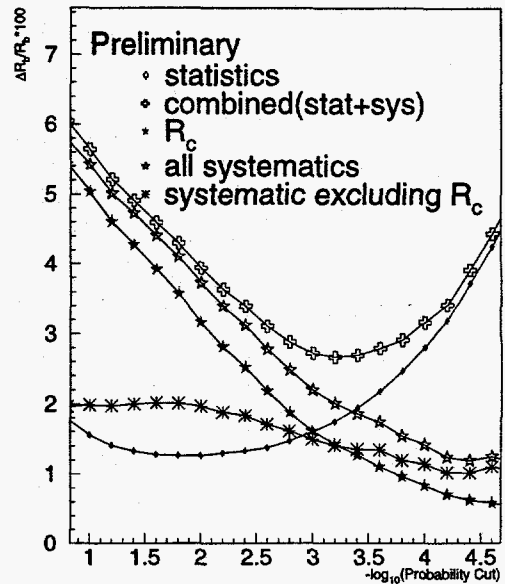


Figure 2: R_b uncertainties versus hemisphere probability cut.

consistent with coming from the primary vertex. A hemisphere is then tagged by requiring that the probability for the hemisphere is below a cut.

Using this tag, the fraction of hemispheres tagged (F_s) and the fraction of events with both hemispheres tagged (F_d) is measured in data. These are combined with the uds hemisphere tagging efficiency (ϵ_{uds}), c hemisphere tagging efficiency (ϵ_c), and b hemisphere correlation (λ_b), estimated from the Monte Carlo, to measure R_b and the b hemisphere tagging efficiency (ϵ_b) simultaneously. These solutions are obtained iteratively from the following expressions:

$$R_b = \frac{(F_s - R_c(\epsilon_c - \epsilon_{uds}) - \epsilon_{uds})^2}{F_d - R_c(\epsilon_c - \epsilon_{uds})^2 + \epsilon_{uds}^2 - 2F_s\epsilon_{uds} - \lambda_b R_b(\epsilon_b - \epsilon_b^2)}, \quad (1)$$

$$\epsilon_b = \frac{F_d - R_c\epsilon_c(\epsilon_c - \epsilon_{uds}) - F_s\epsilon_{uds} - \lambda_b R_b(\epsilon_b - \epsilon_b^2)}{(F_s - R_c(\epsilon_c - \epsilon_{uds}) - \epsilon_{uds})}. \quad (2)$$

The optimal hemisphere probability cut which minimizes the total systematic plus statistical uncertainty in R_b is $10^{-3.2}$. The R_b uncertainties versus the hemisphere probability cut are shown in Fig. 2. At the optimal cut, the result is:

$$R_b = 0.218 \pm 0.004(\text{stat}) \pm 0.004(\text{syst}) \pm 0.003(R_c). \quad (3)$$

The contributions to the systematic uncertainty are shown in Table 1. From Fig. 2 it is clear that the overall systematic uncertainty will decrease with more data.

Detector Systematics			
Systematic	$\delta R_b/R_b$	Systematic	$\delta R_b/R_b$
Efficiency Corrections	0.5%	V^0 Rejection	0.9%
Impact Resolutions	0.5%	Beam Position Tails	0.3%
Physics Systematics			
Systematic	$\delta R_b/R_b$	Systematic	$\delta R_b/R_b$
Correlation Systematics	0.6%	Charm Systematics	1.2%
Light Quark Systematics	0.3%	R_c	1.4%

Table 1: Summary of contributions to the systematic error for probability tag at a cut of $P_{cut} = 10^{-3.2}$

5 A_f from the Left-Right Forward-Backward Asymmetry

Measurements of fermion asymmetries at the Z^0 resonance probe a combination of the vector and axial vector couplings of the Z^0 to fermions, $A_f = 2\nu_f a_f / \nu_f^2 + a_f^2$. The parameters A_f express the extent of parity violation at the $Zff\bar{f}$ vertex and provide sensitive tests of the Standard Model. The tree-level differential cross section for the process $e^+e^- \rightarrow Z^0 \rightarrow ff\bar{f}$ is:

$$\frac{d\sigma_f}{d\cos\theta} \propto (1 - A_e P_e)(1 + \cos^2\theta) + 2A_f(A_e - P_e)\cos\theta, \quad (4)$$

where θ is the outgoing fermion direction with respect to the electron beam and P_e is the electron beam polarization. The parameter A_f can be isolated by forming the left-right forward-backward asymmetry (the double asymmetry):

$$A_{LRFB}^f = \frac{[\sigma_L^f(\cos\theta) - \sigma_L^f(-\cos\theta)] - [\sigma_R^f(\cos\theta) - \sigma_R^f(-\cos\theta)]}{[\sigma_L^f(\cos\theta) - \sigma_L^f(-\cos\theta)] + [\sigma_R^f(\cos\theta) - \sigma_R^f(-\cos\theta)]} = |P_e| A_f \left(\frac{2\cos\theta}{1 + \cos^2\theta} \right) \quad (5)$$

Two analyses are described below. The first measures A_b by using a Momentum Weighted Track Charge technique to determine the direction of the outgoing fermion. The second measures A_c by fully and partially reconstructing $D^{(*)+}$ decays from $Z^0 \rightarrow c\bar{c}$ events.

5.1 A_b from Momentum Weighted Track Charge

A detailed discussion of the Momentum Weighted Track Charge analysis can be found in reference [5]. Basically, the analysis begins by selecting a sample of $Z^0 \rightarrow b\bar{b}$ events and determining the b and \bar{b} directions. A b enriched sample of events is obtained by applying a 2-D impact parameter tag. The event thrust axis \hat{T} , formed from all calorimeter energy clusters, is used to estimate the the direction of the b and \bar{b}

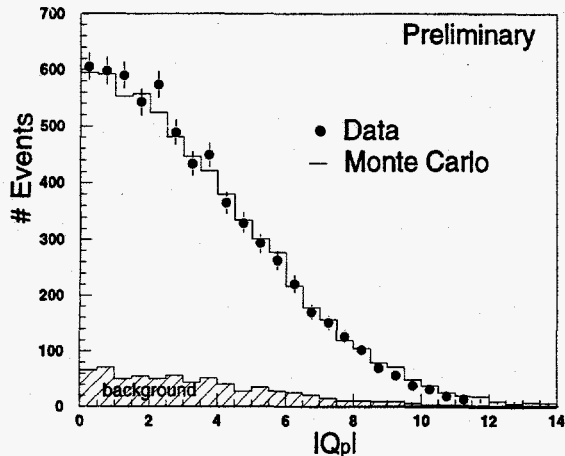


Figure 3: Momentum weighted track charge(Q_p) for data and Monte Carlo.

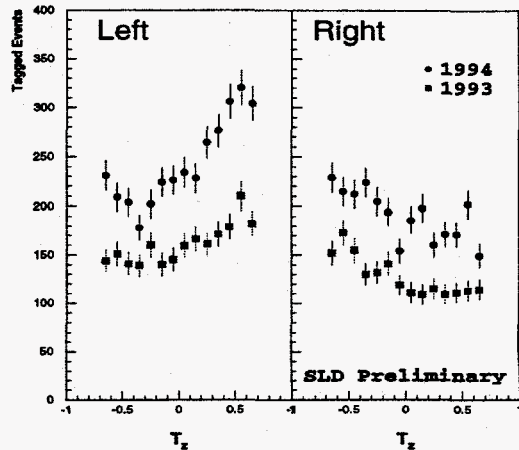


Figure 4: Thrust axis distributions for left and right polarization of the e^- beam signed such that $Q_p < 0$.

quarks. To determine the b quark direction, the Momentum Weighted Track Charge is formed:

$$Q_p = \sum Q_{track} |\vec{p} \cdot \hat{T}|^\kappa \text{sign}(\vec{p} \cdot \hat{T}), \quad \kappa = 0.5. \quad (6)$$

A negative value of Q_p associates the b quark with the forward thrust axis direction ($T_z > 0$). If Q_p is positive then the sign of the T_z is flipped. The distributions of T_z for left and right e^- polarizations are shown in Fig. 4.

The distribution of the Momentum Weighted Track Charge is well reproduced by the Monte Carlo, as shown in Fig. 3. From Monte Carlo, the charged assignment is determined to be correct 69% of the time, giving an analyzing power of $69\% - (100\% - 69\%) = 38\%$. As a cross-check of the analyzing power, the frequency with which the hemispheres of an event agree (P_{agree}) and disagree ($P_{disagree}$) on the direction of the b -quark are calculated. The asymmetry of these quantities ($H = \frac{P_{agree} - P_{disagree}}{P_{agree} + P_{disagree}}$) is proportional to the square of the analyzing power. The measurement of H for the 1993 Monte Carlo, the 1993 data, and the 1993+1994 data are 0.087 ± 0.007 , 0.088 ± 0.016 , and 0.094 ± 0.010 respectively. These are in good agreement with each other and provide confidence in the Monte Carlo estimation of the analyzing power used in obtaining the results for A_b .

The observed left-right forward-backward asymmetry, \bar{A}_i^{obs} (where i represents a bin in T_z), is formed according to equation 5. This observed asymmetry must be corrected for various dilution effects, including the event tag purity, thrust axis smearing, and the analyzing power of the jet charge technique:

$$\bar{A}_i^{corr} = \frac{\bar{A}_i^{obs}}{\Pi_i} - \frac{1 - \Pi_i}{\Pi_i} \bar{A}_i^{udsc}, \quad (7)$$

where Π_i is the $Z^0 \rightarrow b\bar{b}$ purity in bin i , estimated from the Monte Carlo, and \bar{A}_i^{udsc} is the expected asymmetry of light quark events, estimated from the subset of Monte Carlo light quark events which pass the $Z^0 \rightarrow b\bar{b}$ selection.

Systematic Uncertainties	$\frac{\delta A_b}{A_b}$	Systematic Uncertainties	$\frac{\delta A_b}{A_b}$
<i>B</i> -hadron decay & fragmentation	7%	Tracking efficiency / resolution	4%
Light quark subtraction	2%	Beam polarization	2%
<i>B</i> -meson mixing	2%	QCD & other radiative effects	1%
Monte Carlo statistics	6%		
Total			11%

Table 2: Contributions to the A_b systematic uncertainty.

The Monte Carlo distribution of asymmetry is generated with $A_b = 1.0$ and the measured polarization ($P_e^{measured}$) and fitted to the distribution of \tilde{A}_i^{corr} . The lone fit parameter is the measurement of A_b . Using this technique on the 1994 data, a preliminary result of $A_b = 0.79 \pm 0.07(\text{stat}) \pm 0.08(\text{syst})$ is obtained. The contributions to the systematic error are shown in Table 2. Combining the 1994 result with the 1993 result of $0.87 \pm 0.11(\text{stat}) \pm 0.09(\text{syst})$ the preliminary combined result is:

$$A_b = 0.82 \pm 0.06(\text{stat}) \pm 0.08(\text{syst}) \quad (1993 + 1994). \quad (8)$$

5.2 A_c from $D^{(*)+}$ decays

A detailed discussion of the $D^{(*)+}$ analysis can be found in reference [6]. $Z^0 \rightarrow c\bar{c}$ events are identified by fully and partially reconstructing the decays of D^{*+} and D^+ mesons (known collectively as $D^{(*)+}$). The charge of the primary charm quark is uniquely determined by the sign of the $D^{(*)+}$ meson. Event and topology cuts described below are used to reject D 's resulting from $b \rightarrow c$ cascade in $Z^0 \rightarrow b\bar{b}$ events.

The D^{*+} mesons are identified using the decay $D^{*+} \rightarrow \pi_s^+ D^0$, where the D^0 decays via $D^0 \rightarrow K^- \pi^+$ ("3 prong" mode) or $D^0 \rightarrow K^- \pi^+ \pi^0$ ("satellite resonance"). The π_s^+ in the D^{*+} decay is known as the "spectator" pion and carries the sign of the charm quark. The D^+ mesons are identified using the decay $D^+ \rightarrow K^- \pi^+ \pi^-$. Three analyses are followed for reconstructing these decay modes, as discussed below.

5.2.1 Kinematic Analysis for Reconstructing D^{*+}

This method uses standard kinematic cuts to obtain a pure D^{*+} sample. In particular, the higher $x_{D^*} = 2E_{D^*}/E_{CM}$ of the D^{*+} mesons in $c\bar{c}$ events compared to those in $b\bar{b}$ events is used to reject cascade decays. The D^0 , formed from pairs of oppositely charged tracks, is required to have an invariant mass ($M(K^- \pi^+)$) within $1.765 < M(K^- \pi^+) < 1.965 \text{ GeV}/c^2$ for the 3 prong mode and $1.500 < M(K^- \pi^+) < 1.700 \text{ GeV}/c^2$ for the satellite mode. The surviving D^0 candidates are combined with the π_s^+ candidates to form the D^{*+} candidate. This is then required to have an $x_{D^*} > 0.4$.

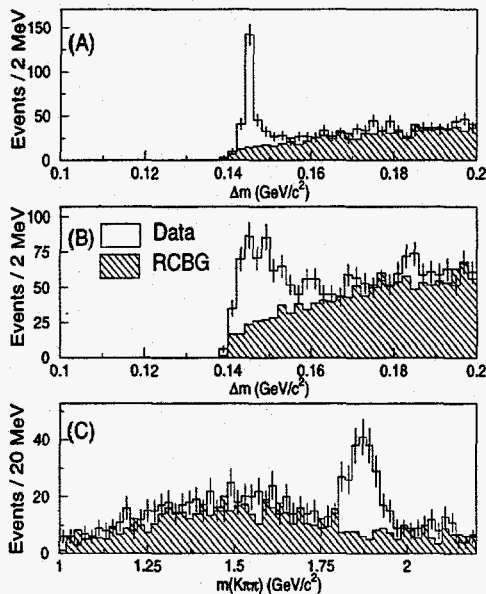


Figure 5: The mass difference between the tagged D^{*+} 's and D^0 's for the 3-prong mode(A) and the satellite mode(B) plus the mass of the $K^-\pi^+\pi^+$ combinations(C) for D^+ decays.

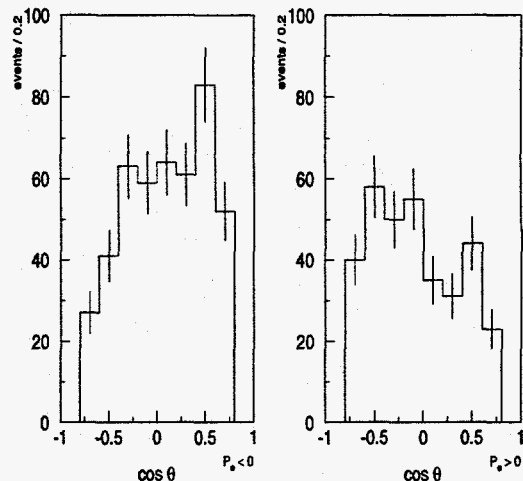


Figure 6: Distribution of the longitudinal component of $D^{(*)+}$ direction for left and right e^- polarizations.

5.2.2 Decay Length Analysis for Reconstructing D^{*+}

The complementary decay length analysis uses a cut on the D^0 's 3-D decay length ($\langle L \rangle \sim 1\text{mm}$) with respect to the primary vertex position and relaxes the kinematic cuts. The decay length significance (L/σ_L) is required to be greater than 2.5. To reduce b contamination, the D^0 is required to point within $20\ \mu\text{m}$ of the primary vertex position in the plane transverse to the beam-line. The D^{*+} candidate is then formed as before and it must satisfy $x_{D^*} < 0.2$.

The overlap in the D^* 's identified by the kinematic and decay length analyses is 28%. The signal is taken from the mass difference (Δm) between the D^{*+} and D^0 . The signal region is ($\Delta m < 0.150\ \text{GeV}/c^2$) and sideband region is ($0.160\ \text{GeV}/c^2 < \Delta m < 0.200\ \text{GeV}/c^2$). The shape of the background spectrum in the signal region is determined from the Monte Carlo. The background normalization is determined by comparing the sideband regions between the data and the Monte Carlo. The purity of the signal ($\frac{f_c}{f_c+f_b}$) is 70% for the 3-prong mode and is 69% for the satellite mode. The distributions for Δm for the 3-prong and satellite modes with the background shape from the Monte Carlo are shown in Fig. 5.

5.2.3 The D^+ Reconstruction Analysis

The precise beam position resolution and decay length resolution are employed to obtain a very pure sample of D^+ decays. In particular, the decay length significance must satisfy $L/\sigma_L > 3.0$, and the D^+ momentum vector must point to within $5(20)$

Systematic Source	δA_c	Systematic Source	δA_c
A_{bkg}	0.032	f_{bkg}	0.032
RCBG x distribution	0.020	RCBG $\cos \theta$ acceptance	0.025
$A_{b \rightarrow D}$	0.023	$f_{b \rightarrow D} / (f_{b \rightarrow D} + f_{c \rightarrow D})$	0.006
$\langle X_c \rangle$	0.018	$\langle X_b \rangle$	0.006
A_e	0.001	Polarization	0.015
$\alpha_s(M_Z^2)$ value	0.004	$o(\alpha_s^2)$ QCD	0.006
fragmentation shape	0.010		
Total		0.066	

Table 3: Contributions to the A_c systematic uncertainty.

mrads of the displacement vector of the vertex to the primary vertex position in the plane transverse(longitudinal) to the beam-line. The D^+ candidate is required to have $x_{D^+} > 0.4$. To reject D^{*+} decays, the mass difference between $M(K^-\pi^+\pi^-)$ and $M(K^-\pi^+)$ must be greater than $0.160 \text{ GeV}/c^2$.

The invariant mass region of $1.800 \text{ GeV}/c^2 < M(K^-\pi^+\pi^+) < 1.940 \text{ GeV}/c^2$ is used for the signal while the regions of $1.640 \text{ GeV}/c^2 < M(K^-\pi^+\pi^+) < 1.740 \text{ GeV}/c^2$ and $2.000 \text{ GeV}/c^2 < M(K^-\pi^+\pi^+) < 2.100 \text{ GeV}/c^2$ are used as sideband regions for estimating the amount of background under the signal. The purity of the signal is 85%. The distribution of $M(K^-\pi^+\pi^+)$ in data with the predicted amount of random combinatoric background from the Monte Carlo is shown in Fig. 5.

5.2.4 Determining A_c

The resulting distributions of $-q \cdot \cos \theta$ for the reconstructed D^{*+} decays, separated for left and right e^- polarizations, are shown in Fig. 6. A_c is extracted from an unbinned maximum likelihood fit based on the tree level cross section for $Z^0 \rightarrow f\bar{f}$. The 1994 preliminary result is $A_c = 0.57 \pm 0.16(\text{stat}) \pm 0.07(\text{syst})$. A summary of the contributions to the systematic error is presented in Table 3. The largest contribution to this error comes from the uncertainty in the amount of background under the signal and the asymmetry of this background. Both will be better determined with more data. Combining the 1993 and 1994 results, we obtain the following preliminary result:

$$A_c = 0.63 \pm 0.13(\text{stat}) \pm 0.07(\text{syst}) \quad (1993 + 1994). \quad (9)$$

6 Precise Measurement of A_{LR}^A

Details of the 1993 A_{LR} measurement are presented in reference [7]. SLD measures the asymmetry of the cross-section for left and right handed electron beam polarizations as shown in Eqn. 10.

$$A_{LR} = \frac{\sigma(e_L^- e^+ \rightarrow Z^0) - \sigma(e_R^- e^+ \rightarrow Z^0)}{\sigma(e_L^- e^+ \rightarrow Z^0) + \sigma(e_R^- e^+ \rightarrow Z^0)} = \frac{2(1 - 4 \sin^2 \theta_W)}{1 + (1 - 4 \sin^2 \theta_W)^2}. \quad (10)$$

This yields a sensitive measure of the weak mixing angle. The measurement is performed on events that have at least 8 calorimeter clusters in $|\cos \theta_{thrust}| < 0.8$ and at least 11 in $|\cos \theta_{thrust}| > 0.8$. This helps to reject $Z^0 \rightarrow e^+ e^-$ events which dilute the asymmetry due to the t-channel diagram. The events must also pass the following cluster energy requirements: $\sum E_{cluster} \geq 0.4 E_{CM}$ where E_{CM} is the center of mass energy measured from the calorimeter; and $|\sum \bar{E}_{cluster}|/E_{total} < 0.6$. These reject backgrounds which are typified by a low mean energy per tower and an imbalance of the energy in the calorimeter due to single beam backgrounds. Monte Carlo studies indicate that the efficiency of this selection for passing Z^0 decays is 93% with a background of $0.25 \pm 0.10\%$.

From 49392 Z^0 's passing event selection, 27225 were left-handed Z^0 's and 22167 were right-handed. This yields a raw asymmetry (A_m) of 0.1024 ± 0.0045 . Combining this with the 1993 average beam polarization $\langle P_e \rangle = (63 \pm 1.1)\%$ one obtains the following result:

$$A_{LR} = A_m / \langle P_e \rangle + (\text{small corrections}) = 0.1628 \pm 0.0071(\text{stat}) \pm 0.0028(\text{syst}). \quad (11)$$

The dominant components of the systematic error are the uncertainties in the Compton Polarimeter laser polarization, and in the correction to the measured polarization caused by the finite energy spread of the electron beam. Both are expected to decrease significantly for data collected after 1993.

This result is corrected to account for photon exchange and for electroweak interference resulting from the deviation of the effective $e^+ e^-$ center-of-mass energy from the Z -pole energy (including the effect of initial state radiation). This yields for the pole asymmetry A_{LR}^o and the effective weak mixing angle:

$$A_{LR}^o = 0.1656 \pm 0.0071(\text{stat}) \pm 0.0028(\text{syst}), \quad (12)$$

$$\sin^2 \theta_W^{eff} = 0.2292 \pm 0.0009(\text{stat}) \pm 0.0004(\text{syst}). \quad (13)$$

This is currently the most precise single measurement of $\sin^2 \theta_W^{eff}$. The total uncertainty is expected to decrease from 0.0010 to 0.0005 with the 1994 data included.

7 Summary

Precision measurements of asymmetries and the b -branching ratio have been made using the SLD. Significant improvements in the precision of these measurement have resulted from the 1994 SLD run. The SLD measurement of A_{LR} is expected to continue to be the single best measurement of the weak mixing angle. The SLD A_b measurement is competitive with LEP measurements and improvements are expected

from utilizing a self calibrating hemisphere technique. The SLD A_c result is already the most precise measurement and will improve with more data. Finally, the SLD R_b measurement is becoming competitive and will improve in precision with more data. All results are in agreement with the Standard Model.

References

- [1] *Polarization at SLC*, M. Woods, Presented at the Eleventh International Symposium on High Energy Spin Physics, SLAC-PUB-6694, (1995).
- [2] *SLD Design Report* G. Agnew *et. al.*, SLAC-0273 (1984).
- [3] *Measurements of R_b using Impact Parameters and Displaced Vertices*, K. Abe *et. al.*, SLAC-PUB-95-6569, (1995).
- [4] ALEPH Collaboration: D. Buskulic *et. al.*, Phys.Lett. **B313**, 535 (1993).
- [5] *Measurement of A_b from the Left-Right Forward-Backward Asymmetry of b -Quark Production in Z^0 Decays using a Momentum Weighted Track Charge Technique*, K. Abe *et. al.*, Phys. Rev. Lett. **74**, 2890 (1995).
- [6] *A Measurement of the Left-Right, Forward-Backward Asymmetry for Charm Quarks with D^{*+} and D^* Mesons*, K. Abe *et.al.*, SLAC-PUB-6681 (1994), submitted to Phys. Rev. Lett.
- [7] *Precise Measurement of the Left-Right Cross-Section Asymmetry in Z Boson Production by e^+e^- Collisions*, K. Abe *et. al.*, Phys. Rev. Lett. **73**, 25 (1994).

DISCLAIMER

This report was prepared as an account of work sponsored by an agency of the United States Government. Neither the United States Government nor any agency thereof, nor any of their employees, makes any warranty, express or implied, or assumes any legal liability or responsibility for the accuracy, completeness, or usefulness of any information, apparatus, product, or process disclosed, or represents that its use would not infringe privately owned rights. Reference herein to any specific commercial product, process, or service by trade name, trademark, manufacturer, or otherwise does not necessarily constitute or imply its endorsement, recommendation, or favoring by the United States Government or any agency thereof. The views and opinions of authors expressed herein do not necessarily state or reflect those of the United States Government or any agency thereof.
